Journal of Bioenergetics and Biomembranes, Vol. 34, No. 1, February 2002 (© 2002)

The Quinol:Fumarate Oxidoreductase From the Sulphate Reducing Bacterium *Desulfovibrio gigas*: Spectroscopic and Redox Studies

Rita S. Lemos,[1] Cláudio M. Gomes,[1] Jean LeGall,[1,2] António V. Xavier,[1] and Miguel Teixeira[1,3]

Received April 4, 2001; accepted May 15, 2001

The membrane bound fumarate reductase (FRD) from the sulphate-reducer *Desulfovibrio gigas* was purified from cells grown on a fumarate/sulphate medium and extensively characterized. The FRD is isolated with three subunits of apparent molecular masses of 71, 31, and 22 kDa. The enzyme is capable of both fumarate reduction and succinate oxidation, exhibiting a higher specificity toward fumarate (K_m for fumarate is 0.02 and for succinate 2 mM) and a reduction rate 30 times faster than that for oxidation. Studies by Visible and EPR spectroscopies allowed the identification of two B-type haems and the three iron–sulphur clusters usually found in FRDs and succinate dehydrogenases: $[2Fe\text{-}2S]^{2+/1+}$ (S1), $[4Fe\text{-}4S]^{2+/1+}$ (S2), and $[3Fe\text{-}4S]^{1+/0}$ (S3). The apparent macroscopic reduction potentials for the metal centers, at pH 7.6, were determined by redox titrations: −45 and −175 mV for the two haems, and +20 and −140 mV for the S3 and S1 clusters, respectively. The reduction potentials of the haem groups are pH dependent, supporting the proposal that fumarate reduction is associated with formation of the membrane proton gradient. Furthermore, co-reconstitution in liposomes of *D. gigas* FRD, duroquinone, and *D. gigas* cytochrome *bd* shows that this system is capable of coupling succinate oxidation with oxygen reduction to water.

KEY WORDS: Fumarate reductase; succinate dehydrogenase; cytochrome *b*; iron–sulphur clusters; *Desulfovibrio*.

INTRODUCTION

Fumarate reductase (FRD) is a membrane bound enzyme that catalyzes the reduction of fumarate to succinate; it plays a key role in the bioenergetic mechanisms of anaerobic cells using fumarate as a terminal electron acceptor. FRD is also capable to catalyze the reverse reaction, succinate oxidation, that is usually catalyzed by succinate dehydrogenase (SDH), a citric acid cycle enzyme that is simultaneously a respiratory complex. Both enzymes share the activity, as well as subunits and cofactor composition (for a review see Hägerhäll, 1997).

The X-ray crystal structures of *Escherichia coli* FRD and *Wolinella succinogenes* FRD (Iverson *et al.*, 1999; Lancaster *et al.*, 1999) confirmed many of the proposed features of these enzymes that have been accumulated by several years of studies, mainly spectroscopic ones, giving an atomic level view of the possible electron transfer pathways. The enzymes are composed of a cytoplasmatic and a transmembrane domain. The cytoplasmatic domain is built of two subunits, a flavoprotein (Frd/SdhA), harbouring the catalytically active FAD, and an iron–sulphur protein (Frd/SdhB), containing a $[2Fe\text{-}2S]^{2+/1+}$, a $[4Fe\text{-}4S]^{2+/1+}$, and a $[3Fe\text{-}4S]^{1+/0}$ cluster. In *E. coli*, the transmembrane domain consists of two polypeptides, with two putative binding sites for menaquinone, while in

Key to abbreviations: FRD, fumarate reductase; SDH, succinate dehydrogenase; NRO, NADH:rubredoxin oxidoreductase; ROO, rubredoxin:oxygen oxidoreductase; DM, *n*-dodecil-β-D-maltoside; PMS, phenazine methosulphate; DTT, dithioerythritol; HQNO, 2-*n*-heptyl-4-hydroxyquinoline-N-oxide; b_H, high potential B-type haem; b_L, low potential B-type haem.

[1]Instituto de Tecnologia Química e Biológica, Universidade Nova de Lisboa, APT 127, 2780-156 Oeiras, Portugal.

[2]Department of Biochemistry and Molecular Biology, University of Georgia, Athens, Georgia 30622.

[3]To whom correspondence should be addressed; e-mail: miguel@itqb.unl.pt.

0145-479X/02/0200-0021/0 © 2002 Plenum Publishing Corporation

W. succinogenes, this domain is built of a single polypeptide, with two B-type haems, named b_H (high potential) and b_L (low potential). There is an experimental evidence in *B. subtilis* that the proximal haem b_P is b_H and the distal haem b_D is b_L (Hägerhäll *et al.*, 1995). The redox cofactors in *W. succinogenes* are arranged in the sequence: FAD–[2Fe-2S]–[4Fe-4S]–[3Fe-4S]–b_H–b_L, separated by 9–17 Å from each other. How the electrons flow between the substrate (succinate or fumarate) and the quinones through these cofactors is still a matter of debate, but it is has been proposed that, in enzymes containing two haems, the distal one (close to the periplasmatic side of the membrane) is the electron donor/acceptor of the quinones (Matsson *et al.*, 2000; Schirawski *et al.*, 1998). It should be mentioned that several enzymes contain only one haem, or even no haem at all (Hägerhäll, 1997), raising the question whether they function in a similar way.

Recently, a new type of SDHs lacking center S3, which is replaced by a second tetranuclear cluster, has been reported in the archaea *Acidianus ambivalens* and *Sulfolobus acidocaldarius* (Gomes *et al.*, 1999; Janssen *et al.*, 1997; Lemos *et al.*, 2001b). Since these SDHs lack a transmembrane anchor, it was proposed that these enzymes are monotopic and interact with the membrane via amphypathic helices (Lemos *et al.*, 2001b).

Sulphate-reducing bacteria of the *Desulfovibrio* genus have an extremely versatile metabolism, with the capability of utilizing several molecules as terminal acceptors in anaerobic respiration, such as sulphate, sulphite, and other sulphur compounds, nitrate, nitrite, and fumarate (e.g. LeGall and Fauque, 1988). In spite of the tremendous amount of work on numerous metalloproteins from *Desulfovibrio* sp., its bioenergetics is still a matter of debate. In particular, very little is known on the membrane-bound proteins from sulphate-reducing bacteria, namely those involved in respiration. So far, only a multihaem cytochrome, containing 16 haems of the C-type (Chen *et al.*, 1994; Pereira *et al.*, 1997), [NiFe] and [NiFeSe] hydrogenases (Fauque *et al.*, 1988; Romão *et al.*, 1997; Teixeira *et al.*, 1987), and the multihaem nitrite/sulphite reductases (e.g., Pereira *et al.*, 1996, 2000) have been isolated from these membranes.

It has been demonstrated that *D. gigas* performs oxidative phosphorylation linked to electron transfer from hydrogen to fumarate (Barton *et al.*, 1970). Quite recently, it was shown that *D. gigas* cells grown on fumarate, besides the fumarate reductase, also express a membrane-bound canonical oxygen reductase, a cytochrome *bd* (Lemos *et al.*, 2001a). This finding suggests that *D. gigas* cells may also be able to respire oxygen or utilize these membrane-bound enzymes to scavenge dioxygen, enabling to sustain the oxygen sensitive respiratory processes, such as sulphate respiration. In order to further understand these highly versatile respiratory processes, an extensive characterization of the membrane-bound complexes in *Desulfovibrio* sp. is essential. Toward this goal, we report the purification and biochemical characterization of FRD from *D. gigas*, the major membrane-bound protein expressed in fumarate grown cells. It is further shown that an electron transfer chain obtained by co-reconstitution in liposomes of *D. gigas* FRD, a quinone, and cytochrome *bd* leads to succinate-driven oxygen consumption.

MATERIALS AND METHODS

Cell Growth and Cell Extracts Preparation

D. gigas cells were grown in two different media: lactate/sulphate (Peck, 1966; LeGall *et al.*, 1965) and fumarate/sulphate. The fumarate/sulphate medium was prepared as described in Miller and Wakerley (1966) using 50 mM sodium fumarate and 50 mM sodium sulphate. Cells were grown in 10-L flasks at 37°C.

The cells were suspended in 10 mM Tris-HCl (pH 7.6) buffer, and broken in a French press at 6000 psi. The suspension was centrifuged at $12{,}000 \times g$ for 1 h in a Beckman J2-MC centrifuge, and the supernatant (cell extract) was centrifuged at $150{,}000 \times g$ for 2 h in a Beckman L8-M ultracentrifuge. The pellet (membrane fraction) was resuspended in 10 mM Tris-HCl (pH 7.6) buffer.

Detergent Extract Preparation

Three different extraction detergents (*n*-dodecil-β-D-maltoside (DM), *N*-dodecyl-*N*,*N*-dimethyl-3-ammonio-1-propane sulphonate (SB12) and Triton X-100) were tested. Each detergent was added to the membranes in the following concentrations: DM in a ratio of 2 g/g of protein, SB12 2% (w/v) and Triton X-100 1% (w/v). The suspensions were stirred for 45 min at 4°C and centrifuged at $160{,}000 \times g$ for 1 h at 4°C. The supernatants are the detergent extracts.

SB12 and Triton X-100 presented low extraction capabilities (only 30 and 50% of the total activity present in the membranes was recovered in the detergent extract), and apparently led to denaturation of the enzyme since the total recovered activity (activity of the detergent extract plus pellet) was only 70%. DM extracted approximately 100% of the total activity present in the membranes, and hence was used for further purification.

Protein Purification

All purification steps were performed on a Pharmacia HiLoad system, at 4°C, and all buffers used contained 0.1% DM and were adjusted to pH 7.6. The DM extract was applied to a Q-Sepharose column XK 26/20 equilibrated with 10 mM Tris-HCl buffer. The column was eluted with a linear gradient of 0–1 M NaCl in the equilibrating buffer and FRD was present in the fraction eluted at 180–200 mM NaCl. This fraction was loaded into an S-200 XK 26/60 column and eluted with 10 mM Tris-HCl/150 mM NaCl. The purification steps were followed by UV–Visible spectroscopy and FRD activity. Approximately 10 mg of pure protein (as judged by sodium dodecyl sulfate-polyacrylamide gel electrophoresis (SDS-PAGE)) were obtained from 200 g of cells (wet weight).

Biochemical Procedures

Protein concentration was determined by a modified microbiuret method for membrane proteins (Waters, 1978).

Haem content was determined by pyridine-haemochrome using the molar absorptivity $\varepsilon_{\text{R-O,556–540}} = 23.98\ \text{mM}^{-1}\ \text{cm}^{-1}$ for the B-type pyridine-haemochrome (Berry and Trumpower, 1987), and by reduced minus oxidized spectra using a molar absorptivity of $\varepsilon_{\text{R-O,562–577}} = 22\ \text{mM}^{-1}\ \text{cm}^{-1}$ for a B-type haem.

Labile iron content was chemically determined by the 2,4,6-tripyridyl-s-triazine (TPTZ) method (Fischer and Price, 1964).

Molecular masses of the protein complex were determined by 5–20% acrylamide, 0–15% sucrose SDS-PAGE. Prior to loading in the gel the samples were incubated for 30 min in the loading buffer containing 8 M urea (Hames, 1990). Proteins were stained with Coomassie brilliant blue (Diezel *et al.*, 1972).

Benzyl viologen:fumarate oxidoreductase activity was measured following the benzyl viologen absorbance decrease at 578 nm ($\varepsilon = 7.8 \times 10^3\ \text{M}^{-1}\text{cm}^{-1}$). The enzyme sample was added to an anaerobic solution containing 50 mM potassium phosphate (pH 7.6)/0.1% DM buffer, and 0.3 mM benzyl viologen. The dye was reduced with a sodium dithionite solution (50 mg/mL) until the optical density reached approximately 2 and the reaction was started by the addition of 20 mM disodium fumarate (Spencer and Guest, 1973).

Rate of *quinol:fumarate oxidoreductase* activity was measured with the use of the menaquinol analogue plumbagin (5-hydroxy-2-methyl-1,4-napthtoquinone). Reduced plumbagin was prepared by exposing a 20 mM ethanolic solution, in acidic conditions (HCl), to metallic zinc. Assays were carried out anaerobically in 100 mM potassium phosphate (pH 7.6)/0.1% DM buffer containing 20 mM dissodium fumarate and 0.2 mM of reduced plumbagin. The activity was monitored by following quinol absorbance decrease at 341 nm ($\varepsilon = 8.7\ \text{mM}^{-1}\ \text{cm}^{-1}$) (Rothery *et al.*, 1999).

Succinate:DCPIP oxidoreductase activity was monitored by following the PMS-coupled reduction of DCPIP at 578 nm ($\varepsilon = 21 \times 10^3\ \text{M}^{-1}\ \text{cm}^{-1}$). The reaction mixture contained 80 mM potassium phosphate (pH 7.6)/ 0.1% DM buffer, 0.36 mM PMS, and 0.36 mM DCPIP. The reaction was started by the addition of succinate (Samain *et al.*, 1987).

Succinate:quinol oxidoreductase activity was measured following the reduced plumbagin absorbance increase at 341 nm. Assays were carried out anaerobically in 100 mM potassium phosphate (pH 7.6)/0.1% DM buffer containing 20 mM succinate and 0.2 mM of reduced plumbagin.

Oxygen consumption was measured polarographically at 30°C with a Clark type oxygen electrode (YSI Mode 5300, Yellow Springs). Assays were carried out in a microchamber (600 μL). The turnover number was calculated assuming that the concentration of O_2 in air-saturated buffer at 30°C is 223 μM.

Reconstitution experiments: Asolectine (32 mg), 460 μL of octyl glucoside (0.5 M), and 0.7 mg of duroquinone were solubilized in 4 mL of HEPES buffer (200 mM), by sonication. The proteins (5 μM cytochrome *bd* and 15 μM of FRD, final concentration) were added to this suspension and stirred in the presence of biobeads (Biorad), for detergent removal, for approximately 4 h. Cytochrome *bd* was purified as in Lemos *et al.*, 2001a. The quinone was kept reduced by 5 mM DTT.

Spectroscopic Techniques

UV–Visible spectra were obtained on a Shimadzu UV-1630 spectrophotometer, equipped with a temperature controller and a stirring system. Visible spectra at liquid nitrogen temperature were recorded on an OLIS DW2 spectrophotometer. Visible spectra data were analyzed using the MatLab™ software. EPR spectra were recorded on a Bruker ESP 380 spectrometer equipped with an ESR900 continuous-flow helium cryostat from Oxford Instruments.

N-terminal Sequencing

The protein subunits were first separated in a 5–20% acrylamide and 0–15% sucrose SDS-PAGE gel and electroblotted to PVDF membranes as described in Choli

and Withmann-Liebold, 1990. The N-terminal sequence was determined by the method of Edman and Begg (1967), using an Applied Biosystem Model 477A protein sequencer.

Redox Titrations

The reduction potentials of the haems were determined by titrations monitored by visible spectroscopy. The enzyme, as isolated, was titrated under anaerobic conditions (Argon is continuously fluxed into the cuvette), at room temperature at different pH values (6.5, 7, 7.6, 7.9, 8.2, and 8.5) in 100 mM MES-bisTris buffer with 0.1% DM. The following redox mediators were used, each at a final concentration of 0.75 μM: 1,2 naphthoquinone, phenazine methosulphate, 1,4-naphthoquinone, methylene blue, duroquinone, menadione, plumbaguin, phenazine, 2-hydroxy-1,4-naphthoquinone, phenosafranine, and neutral red. The iron–sulphur clusters reduction potentials were determined by redox titrations monitored by EPR spectroscopy. The enzyme was also titrated under anaerobic conditions, at room temperature and in 10 mM Tris-HCl (pH 7.6 buffer). The following redox mediators were used, each at a final concentration of 20 μM: trimethylhydroquinone, phenazine methosulphate, 1,4-naphthoquinone, 5-hidroxy-1, 4-naphthoquinone, duroquinone, indigo tetrasulfonate, indigo trisulfonate, indigo disulfonate, 2-hidroxy-1, 4-naphthoquinone, anthraquinone 2,7-disulfonate, anthraquinone 2-sulfonate, safranine, and neutral red.

The reduction potential was varied by stepwise additions (approximately 1 μL) of 1 or 5 mg/mL sodium dithionite anaerobic solutions and was measured with a silver/silver chloride combined electrode, calibrated against a saturated quinhydrone solution (pH 7), and by performing redox titrations of horse cytochrome *c*. The potentials are quoted in relation to the standard hydrogen electrode.

RESULTS AND DISCUSSION

FRD Induction

D. gigas cells grown in the standard lactate/sulphate medium express low levels of SDH/FRD, but when grown in the presence of fumarate, a large increase in B-type haem content occurs (Fig. 1 traces a and b), as previously observed (Hatchikian and Legall, 1972). Accordingly, the FRD specific activity in the membranes of the fumarate grown cells is 25 times higher than when the cells are grown in lactate/sulphate, indicating induction of FRD when cell growth is performed in the presence of fumarate.

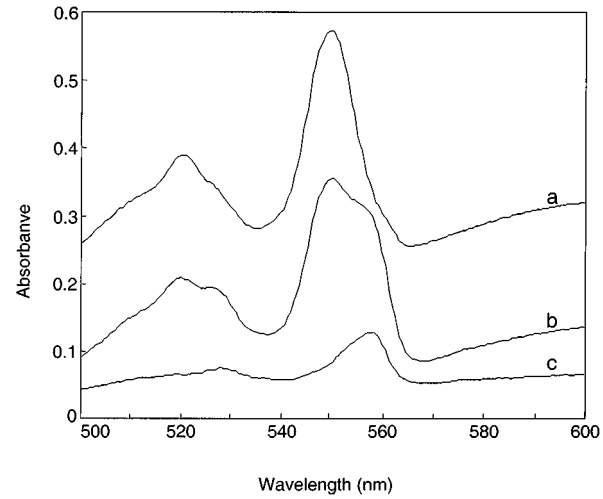

Fig. 1. Reduced minus oxidized visible spectra of *D. gigas* membranes, at liquid nitrogen temperature (77 K). Trace a: lactate/sulphate grown, reduced with dithionite. Trace b: fumarate/sulphate grown, reduced with dithionite. Trace c: fumarate/sulphate grown, reduced with succinate.

Characterization of the Detergent Extract

To determine whether the protein maintained its integrity during purification, a partial characterization of FRD in a most intact form (detergent extract) was performed. The Visible redox spectrum of *D. gigas* membrane extract is dominated by features typical of low spin C- and B-type haems (Fig. 1, trace b). Addition of succinate to the extract (as well as to the crude membranes) leads to a reduction of ~40–45% of the B-type haems, which indicates that the enzyme is active and that the substrate is able to reduce the b_H (Fig. 1, trace c); almost no reduction of the C-type haems was achieved, which is in agreement with the redox potentials of most C-type cytochromes found in *Desulfovibrio* species (e.g., Pereira *et al.*, 1998). Plumbagin (a quinone) reduced 50% of the B-type haems of the extract (b_H), but menadiol reduced only 20% of these haems, probably because of a lower affinity to the quinol-binding site compared with reduced plumbagin. These quinones also reduce a small fraction of cytochromes *c*.

The DM detergent extract was titrated at room temperature and pH 7.6. The experimental data for the B-type haems (monitored at 561 nm) was fitted with two Nernst curves, indicating the presence of two different haems, with apparent reduction potentials of -45 and -190 mV (data not shown). The data for the C-type haems (followed at 552 nm) was analyzed in order to achieve a macroscopic description of their behavior; the experimental data was fitted with the sum of five Nernst curves and the reduction potentials ranged from -30 to -350 mV (data not

shown), values very similar to those of the high molecular mass 16-haem cytochrome (Chen *et al.*, 1994; Pereira *et al.*, 1997).

Kinetic Characterization

The K_m and V for fumarate were determined in the membrane extracts from cells grown in fumarate/sulphate and lactate/sulphate: $K_m = 0.015$ mM; $V = 0.27$ U/mg and $K_m = 0.0064$ mM; $V = 0.069$ U/mg, respectively. These differences in the kinetic parameters indicate that different enzymes may be expressed by varying the growth conditions as observed in other organisms, such as *E. coli* (Wallace and Young, 1977; Hirsch *et al.*, 1963).

Enzyme Biochemical Characterization

Purification

The membrane fraction comprises 85% of the total fumarate reductase activity found in the crude extract. The purification procedure used was able to purify the enzyme 11 times with a recovery of 50% of the activity present in the membranes. The purity of the sample was assessed by SDS-PAGE. The three bands corresponding to the apparent molecular masses of 71, 31, and 22 kDa were blotted to PVDF membranes and, as expected, were identified as FrdA, FrdB, and FrdC, respectively, by their N-terminal sequence (Fig. 2).

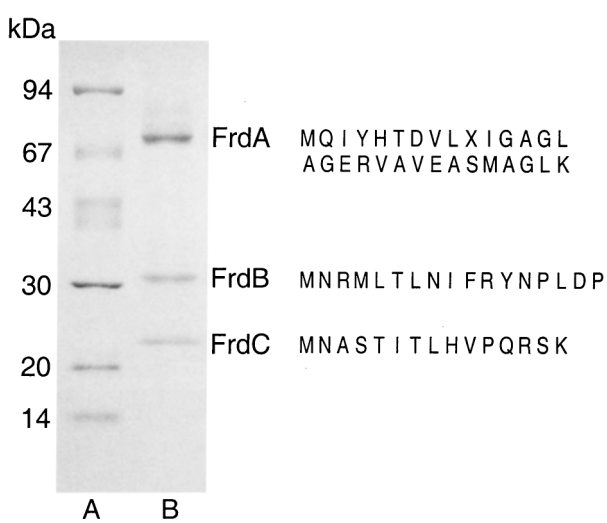

Fig. 2. Sodium dodecyl sulfate-polyacrylamide gel electrophoresis (SDS-PAGE) of FRD from *D. gigas*. Lane A: molecular mass markers and Lane B: FRD form *D. gigas* as isolated (~2 μg). The N-terminus aminoacid sequence of each band is also presented.

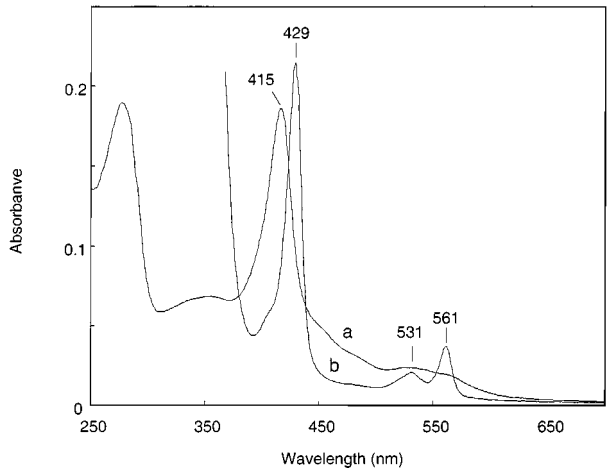

Fig. 3. UV–Visible spectra of *D. gigas* FRD, pH 7.6 at room temperature: (a) oxidized and (b) dithionite reduced.

Spectroscopic Characterization

UV–Visible Spectroscopy. The UV–Visible spectra of the purified enzyme exhibits features characteristic of B-type haems (see Fig. 3), which were identified by the pyridine-haemochrome spectrum (alfa peak at 555 nm, data not shown). The ratio between labile iron and haem (determined by the TPTZ method and redox visible spectra, respectively) was 9:2, which is compatible with the presence of two B-type haems and the three canonical iron–sulphur clusters present in most FRD/SDH (Hägerhäll, 1997). The FAD and the iron–sulphur clusters are only observable as a broad band at ~450 nm underneath the intense Soret band.

Addition of succinate to the purified enzyme leads to a reduction of up to 40% of the haems in relation to dithionite reduction, which allows to compare the optical properties of the b_H and b_L: the α band of b_H is red shifted 1.5 nm and the Soret band is sharper and has a small red shift of 0.5 nm in relation to b_L (data not shown).

2-*n*-Heptyl-4-hydroxyquinoline-N-oxide (HQNO), a potent ubiquinone and menaquinone antagonist, acts on many respiratory enzymes containing cytochrome *b* and quinol binding sites. The HQNO effect on the B-type haems from *D. gigas* is similar, but at a lesser extent, than that observed for *Bacillus subtilis* SDH (Smirnova *et al.*, 1995). The spectral effect of HQNO suggests that the inhibitor binds near one of the FRD haems (data not shown).

EPR Spectroscopy

In the magnetic field region of 30–40 mT the EPR spectrum of the oxidized enzyme exhibits only

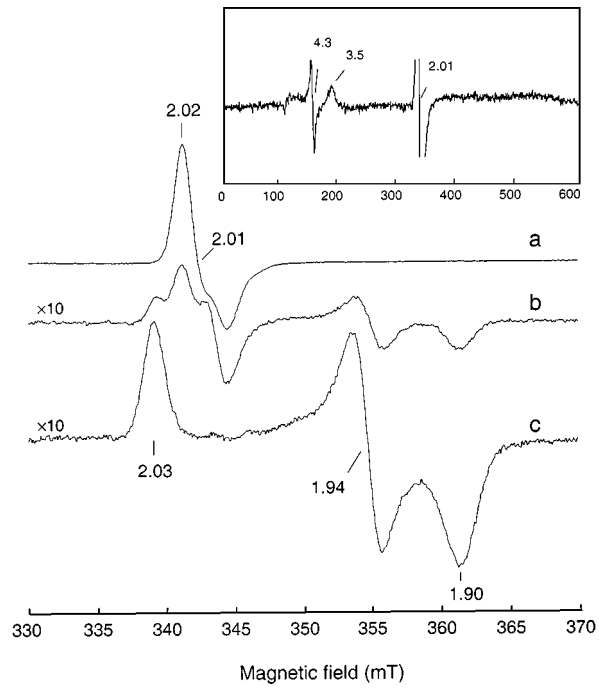

Fig. 4. EPR spectra of *D. gigas* FRD. Trace a: as isolated (oxidized), trace b: reduced with succinate, and trace c: reduced with deazoflavin. Inset: EPR spectra of the native protein in the field region of 10–600 mT. Microwave power: 2.4 mW, modulation amplitude: 0.9 mT; microwave frequency: 9.64 GHz, and temperature: a, inset: 8 K and b,c: 15 K.

the resonances of the oxidized S3 center ([3Fe-4S]$^{1+/0}$), at $g_{max} = 2.02$ (Fig. 4, trace a). In the wide region of 10–600 mT, two more resonances could be detected: a minor intensity signal at $g = 4.3$ attributed to rhombic iron III (nonspecific iron) and another at $g_{max} = 3.5$, characteristic of low spin ferric haems with an axial ligand field (Fig. 4 inset). Within experimental resolution, both haems have the same strong g_{max} type spectrum, in agreement with the similar relative orientations of the histidine imidazoles at the two haems (Lancaster *et al.*, 1999); the angle between the imidazole planes, $\sim 90^{\circ}$, results in a quasi-axial ligand field at the haem iron, as confirmed by the EPR g-values. The intensity of the S3 EPR signal decreased after the anaerobic addition of succinate, as did the $g = 3.5$ resonance (data not shown) and another set of resonances develops at $g = 2.03$, 1.94, and 1.90 (Fig. 4, trace b). This signal was observed optimally at approximately 20 K, but remained detectable up to liquid nitrogen temperature, a behavior typical of [2Fe-2S]$^{2+/1+}$ reduced clusters, and was assigned to center S1. Upon reduction with illuminated deazoflavin the [3Fe-4S]$^{2+/1+}$ cluster signal completely disappeared, the amplitude of the [2Fe-2S]$^{2+/1+}$ cluster resonance fully develops (Fig. 4, trace c) and new signals were not observable. The microwave power saturation behavior of the reduced [2Fe-2S]$^{2+/1+}$ cluster in succinate-, dithionite-, and deazoflavin-reduced states suggests a magnetic interaction with another center, most probably the reduced [4Fe-4S]$^{1+}$ cluster. Under nonsaturation conditions, double integration of the resonances of center S3 (fully oxidised sample) and center S1 (fully reduced sample) yields a 1:1 ratio, showing a stoichiometric content of these two clusters. Even at low temperatures and high microwave power, no other resonance due to cluster S2 could be observed; its presence could only be inferred from its effect, upon reduction, on the relaxation behavior of center S1.

Unlike what is observed in *E. coli* SDH (Rothery and Weiner, 1998), HQNO had no effect on the [3Fe-4S]$^{1+}$ cluster signal.

Kinetic Studies

As expected for a FRD, the determined K_m for fumarate was lower than for succinate: 0.02 mM and 2 mM, respectively (the K_m for fumarate is quite close to that determined on the detergent extract). The rate of fumarate reduction was approximately 30 times higher than for succinate oxidation (45 U/mg for fumarate reduction and 1.4 U/mg for succinate oxidation). The quinol:fumarate oxidoreductase and succinate:quinol oxidoreductase activities of the enzyme (0.7 U/mg and 2.2 U/mg, respectively) were not inhibited by HQNO, up to the concentration of 20 μM.

The redox titration of the haems at pH 7.6 (see below) was also performed in the presence of HQNO. Unlike *B. subtilis* SDH (Smirnova *et al.*, 1995) no alteration of the apparent reduction potentials was observed. All the experimental data obtained with HQNO indicate that the quinone-binding site of *D. gigas* may be different from that of *B. subtilis.*

Co-Reconstitution of *D. gigas* FRD and Cytochrome *bd*

D. gigas membranes are able to consume oxygen with a respiratory rate of 2.9 nmol O_2 (min mg)$^{-1}$, when succinate is used as electron donor; this value is of the same order of magnitude of that measured in the membranes of some aerobic bacteria (e.g., *Rhodothermus marinus* (Pereira *et al.*, 1999): 1.5 nmol O_2 (min mg)$^{-1}$). The membranes of *D. gigas* cells grown in the standard lactate/sulphate medium present respiratory rates considerably lower (0.37 nmol O_2 (min mg)$^{-1}$) than those obtained from the fumarate/sulphate growth (Lemos *et al.*,

2001a). A membrane-bound terminal oxygen reductase, of the cytochrome *bd* family, was purified from *D. gigas* and characterized (Lemos *et al.*, 2001a). In the presence of sonicated lipids and duroquinone (shown to be the most efficient artificial electron donor to cytochrome *bd*), the enzyme is capable of reducing oxygen to water with a turnover number of 3.5 s^{-1}. An *in vitro* reconstitution of an electron transfer chain was successively achieved by co-reconstitution of *D. gigas* FRD and cytochrome *bd*, in asolectin liposomes, in the presence of duroquinone (see Materials and Methods section). Upon the addition of succinate, an oxygen consumption rate of 0.25 s^{-1} was obtained. It should be stressed that this rate was obtained with a nonphysiological quinone, which in part may explain it's low value. Nevertheless, this shows qualitatively, that *D. gigas* cells in the presence of fumarate/succinate may also respire or detoxify oxygen, by using a membrane bound respiratory chain. This process may work in parallel with that occurring in the cytoplasm, involving NADH:rubredoxin oxidoreductase, rubredoxin, and rubredoxin:oxygen oxidoreductase (Chen *et al.*, 1993; Gomes *et al.*, 1997; Frazão *et al.*, 2000), which couples NADH oxidation to the reduction of oxygen to water. These two oxygen consumption processes may contribute to the capability of *D. gigas* to survive in toxic environments.

Redox Characterization

The reduction potentials of the $[2Fe\text{-}2S]^{2+/1+}$ and $[3Fe\text{-}4S]^{1+/0}$ clusters were determined by redox titrations at pH 7.6, monitored through EPR spectra at 10 K. The apparent reduction potential determined for the $[3Fe\text{-}4S]^{1+/0}$ center was +20 mV (Fig. 5A). Below −120 mV the potential of the titrated solution became unstable and this resulted in a lack of experimental data near the redox transition of the $[2Fe\text{-}2S]^{2+/1+}$ cluster; nevertheless, it was possible to estimate its value as -140 ± 20 mV (data not shown). Higher concentrations of mediators or addition of substrate did not improve the redox equilibrium with the electrode. The reduction potential for the $[4Fe\text{-}4S]^{2+/1+}$ center could not be determined since it is not EPR detectable under the experimental conditions used. In general, these centers have potentials lower than −200 mV (Hägerhäll, 1997).

The reduction potentials of the haems were determined by titrations monitored by Visible spectroscopy at room temperature and at different pH values. The apparent macroscopic potentials, determined at pH 7.6 using independent Nernst curves ($n = 1$) with E_0 of −45 and −175 mV, are in agreement with the values obtained in the detergent extract, a more intact form of the enzyme, at the same pH (Fig. 5A). However, the best fitting with independent Nernstian curves give consistent nonrandom residuals that imply different haem contributions at all pH values lower than 7.9 (see Table I; at pH 7.6 the haems b_L and b_H have 55 and 45% contributions, respectively) indicating that redox interactions should be taken into consideration. Indeed, according to the structural data of *W. succinogenes* FRD, the distance between the haem irons is 15.6 Å (Lancaster *et al.*, 1999, 2000). Using Coulomb's law and the consensus effective dielectric constant of 15 (Bertini*et al.*, 1997; Soares *et al.*, 1997), this distance leads to a direct electrostatic interaction of 58 mV. Defining as the reference state the fully reduced enzyme, the microscopic potential (e_m) is that of a center when all other centers are also reduced (Turner *et al.*, 1996). Thus, a positive interaction potential between two centers implies that when one center becomes oxidized, the other center becomes more difficult to oxidize (i.e. its redox potential increases). However, direct electrostatic contributions can be partially or totally overridden (or overaccentuated) by redox-linked structural modifications that add a mechanochemical contribution to the interaction energies (Xavier, 2000; Louro, *et al.*, 2001). Since the haem spectra cannot be resolved, it is not possible to follow the individual microstates along the redox titration curves. Thus, only macroscopic reduction potentials for the ensemble of the two haems can be determined by direct analysis of the redox titration curves. In order to obtain the microscopic redox potentials of each haem (the only parameters that can be directly correlated with the structure (Brennan *et al.*, 2000), further information is needed. A similar situation may apply for the other redox centers of this enzyme, located at approximately 12 Å from each other (Iverson *et al.*, 1999; Lancaster *et al.*, 1999).

Although there is not a sufficient number of independent data to determine all the interaction potentials,

Table I. Experimental Reduction Potentials of b_H and $b_L$at Different pH Values

pH values	Reduction potentials b_H	Reduction potentials b_L	Haem contribution[a] (b_H/b_L)
6.50	10	−130	0.7
7.00	0	−150	0.8
7.60	−45	−170	0.8
7.87	−60	−190	0.8
8.17	−60	−185	1.0
8.50	−60	−190	1.0

[a] Using two independent Nernst curves ($n = 1$), different contributions have to be assigned to each haem (see text).

including redox and redox-Bohr interactions (see below), and hence the individual microscopic potentials, some values can be estimated by a close examination of the available experimental data for the three component system comprising b_L, b_H, and S3. Because of the relative distances between the centers, interactions were considered only between the two haems and between haem b_H and the trinuclear center. With this simplified model, the pH dependent "microscopic" potential of haem b_L at pH 7.6 is uniquely determined as -175 mV; on the contrary, the potential for haem b_H is significantly dependent on the value of the interaction potential. Indeed, when the redox interaction between the haem b_H and the trinuclear center (S3) is considered null, any value for the redox interaction b_L–b_H between 0 and 90 mV, with a concomitant changing of the microscopic redox potential of b_H, from -45 to -140 mV, respectively, allows fittings of similar quality of the experimental haem titration. However, the deviation from a 1:1 ratio observed using two independent Nernst equations also occurs in these simulations (see above). This is to be expected since the observed deviation can never be explained due to the reciprocity of the redox interactions between the two haems. Indeed this is only compatible with a negative cooperativity between the haem that contributes to the component with the lower ΔOD (i.e. haem b_H) and a third center (i.e. S3). Accordingly, a much better fit of the experimental haem titration curve is obtained if a redox interaction, I_{b_H-S3}, is introduced. This is illustrated for pH 7.6 in Fig. 5 (B) where $I_{m\,b_H-S3} = +30$ mV, $e_{m\,S3} = -10$ mV, and $e_{m\,b_H} = -60$ mV and $e_{m\,b_L} = -175$ mV. As mentioned above, a unique solution cannot be obtained at this stage; however, it becomes clear that redox interactions between the FRD/SDH centers should be considered.

Both redox transitions of the haems depend on the pH (see Tables I and II), i.e. show a clear redox-Bohr effect (Papa, 1979; Louro *et al.*, 1996). Assuming a simple ionization equilibrium, the pK_a^{ox} and pK_a^{red} were calculated by Eq. (1):

$$E = E_A + \frac{RT}{F} \ln\left(\frac{K_a^{red} + [H^+]}{K_a^{ox} + [H^+]}\right) \qquad (1)$$

which yields $pK_a^{ox} \leq 6.00$ for both b_L and b_H, a $pK_a^{red} = 8.1 \pm 0.1$ for b_H and a $pK_a^{red} = 7.7 \pm 0.6$ for b_H (Table II and Fig. 6). These values are well between the physiological pH range, but as it was not possible to perform titrations at lower pH values only upper limits for the pK_a^{ox} could be obtained.

The structural data on *W. succinogenes* FRD shows that the haem propionates are not hydrogen bonded to protolytic residues (Lancaster *et al.*, 1999). Hence, the pH dependence of the reduction potentials may be due to a direct protonation event at the haem propionates; interestingly, analysis of the X-ray structure of the oxidized *W. succinogenes* FRD (Lancaster *et al.*, 1999) shows that

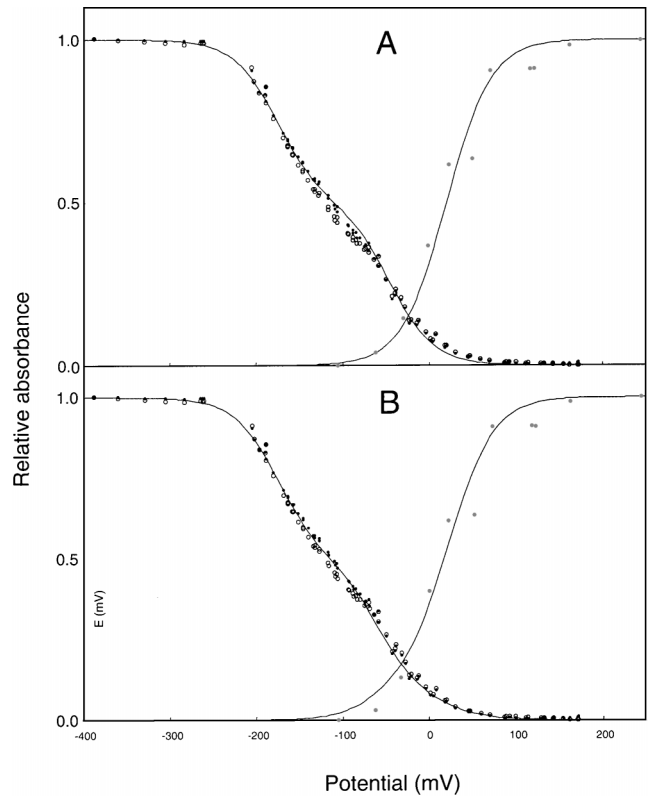

Fig. 5. Redox titrations of *D. gigas* FRD at pH 7.6. Titration of the B-type haems, followed by UV–Visible spectroscopy at 430 nm (●) and 561 nm (○) and titration of the S3 cluster (◍) followed by EPR spectroscopy. The [3Fe-4S] cluster was followed at $g = 2.02$. Panel A: The apparent macroscopic potentials for the B-type haems was determined using independent Nernst curves ($n = 1$) with E_0 of -45 and -175 mV with different haem contributions of 45 and 55% for haems b_H and b_L, respectively. For the S3 cluster a Nernst curve ($n = 1$) with E_0 of $+20$ mV was used. Panel B: The microscopic potential used were $e_{mS3} = -10$ mV, $e_{m\,b_H} = -60$ mV, and $e_{m\,b_L} = -175$ mV, considering $I_{m\,b_H-S3} = +30$ mV and $I_{m\,b_H-b_L} = 0$ mV.

Table II. Reduction Potentials and pK_a Values for the Oxidised and Reduced Forms of Haems b_H and b_L

	Reduction potentials		pK_a values	
	E_0^A	E_0^B	pK_a^{ox}	pK_a^{red}
b_H	≥50	−74	≤6.0	8.1
b_L	≥−95	−195	≤6.0	7.7

Note. E_0^A and E_0^B are the potentials for the acidic and basic forms respectively.

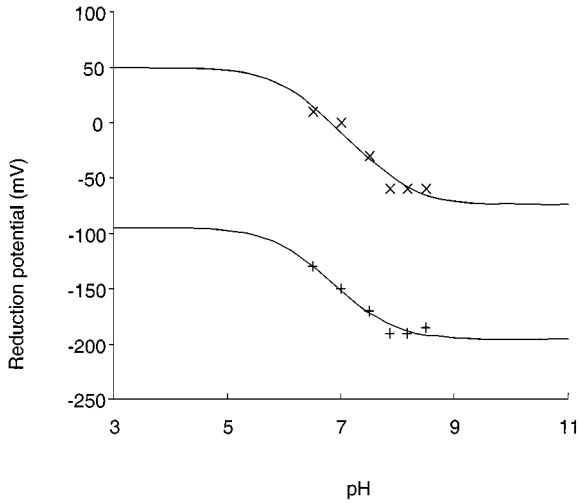

Fig. 6. pH dependence for the reduction potential of the B-type haems from *D. gigas* FRD. The solid lines correspond to curves calculated using Eq. (1) with pK_a^{ox} and pK_a^{red} from Table II.

one of the propionates of haem b_L is hydrogen bonded to an arginine, a situation similar to that of the haem *a* in haem-copper cytochrome oxidases (Tsukihara *et al.*, 1995; Iwata *et al.*, 1995). This redox-Bohr behavior, which is also observed in SDHs (Fernandes *et al.*, in press), may be physiologically relevant as it was recently shown that menaquinone interacts close to haem b_D, releasing its protons into the periplasm, possibly by involving a glutamate residue which forms part of the quinone binding pocket (Lancaster *et al.*, 2000). Thus, haem b_L may act simultaneously as electron and proton acceptor of the quinol, behavior important for the proton translocation by these enzymes (Schirawski and Unden, 1998).

In spite of the putative binding of the quinol close to the low-potential haem, its involvement in the intramolecular electron transfer chain of FRD (or SDH) has been questioned, as its reduction potential is apparently lower than that of the electron donating quinol. Firstly, it should be stressed that the actual potential of the bound quinol is not known (for example, considerable changes of more than 50 mV have been measured upon binding of quinols to cytochrome *bd* (Hastings *et al.*, 1998)). Secondly, the same apparent uphill electron transfer happens with the S2 cluster, which has a potential quite lower (<-200 mV) than its immediate neighbors, the S1 and S3 centers. As for the S2 cluster, the low value of the haem b_L redox potential is fully compatible with its involvement in electron transfer between the quinol and haem b_H, just ensuring electron transfer between the quinol and b_H, which are too far apart for this process to be catalytically competent (Ohnishi *et al.*, 2000; Page *et al.*, 1999). Moreover, its low potential contributes to further warrant directionality of the electron flow, as it will be immediately reoxidized by haem b_H, thus becoming available to receive the second electron from the semiquinone formed in the first step. The same reasoning may apply for the subsequent electron transfer steps, from haem b_H to the $[3Fe\text{-}4S]^{1+/0}$ center and so on until the flavin moiety, and can similarly explain the electron transfer steps for the reverse reaction (oxidation of succinate).

In conclusion, the spatial and thermodynamic properties of the redox centers in the dihaemic fumarate/succinate oxidoreductases is such that optimally couples the initial and final two-electron steps to the directionality of electron transfer along the enzyme subunits and across the membrane.

ACKNOWLEDGMENTS

This work was supported by FCT-Portugal Grants 36560/99 and 36558/99 to Miguel Teixeira. Rita S. Lemos is recipient of PRAXIS XXI Grant BD/19867/99.

REFERENCES

Barton, L. L., LeGall, J., and Peck, H. D. (1970). *Biochem. Biophys. Res. Commun.* **41**, 1036–1042.
Berry, E. A., and Trumpower, B. L. (1987). *Anal. Biochem.* **161**, 1–15.
Bertini, I., Gori-Savellini, G., and Luchinat, C. (1997). *J. Biol. Inorg. Chem.* **2**, 114–118.
Brennan, L., Turner, D., Messias, A., Teodoro, M., LeGall, J., Santos, H., and Xavier, A. V. (2000). *J. Mol. Biol.* **298**, 61–82.
Chen, L., Liu, M.-Y., LeGall, J., Fareleira, P., Santos, H., and Xavier, A. V. (1993). *Biochem. Biophys. Res. Commun.* **193**, 100–105.
Chen, L., Pereira, M. M., Teixeira, M., Xavier, A. V., and LeGall, J. (1994). *FEBS Lett.* **347**, 295–299.
Choli, T., and Withmann-Liebold, B. (1990). *Electrophoresis* **11**, 562–568.
Diezel, W., Kopperschläger, G., and Hoffmenn, E. (1972). *Anal. Biochem.* **48**, 621–623.
Edman, P., and Begg, G. (1967). *Eur. J. Biochem.* **1**, 80–90.
Fauque, G., Peck, H. D., Moura, J. J., Huynh, B. H., Berlier, Y., DerVartanian, D. V., Teixeira, M., Przybyla, A. E., Lespinat, P. A., Moura, I., and LeGall, J. (1988). *FEMS Microbiol.* **4**, 299–344.
Fernandes, A. S., Pereira, M. M., and Teixeira, M. (2001). *J. Bioenerg. Biomemb.* **33**, 343–352.
Fischer, D. S., and Price, D. C. (1964). *Clin. Chem.* **10**, 21–25.
Frazão, C., Silva, G., Gomes, C. M., Matias, P., Coelho, R., Sieker, L., Macedo, S., Liu, M. Y., Oliveira, S., Teixeira, M., Xavier, A. V., Rodrigues-Pousada, C., Carrondo, M. A., and LeGall, J. (2000). *Nat. Struct. Biol.* **7**, 1041–1045.
Gomes, C. M., Lemos, R. S., Teixeira, M., Kletzin, A., Huber, H., Stetter, K. O., Schäfer, G., and Anemüller, S. (1999). *Biochem. Biophys. Acta* **1411**, 134–141.
Gomes, C. M., Silva, G., Oliveira, S., LeGall, J., Liu, M. Y., Xavier, A. V., Rodrigues-Pousada, C., and Teixeira, M. (1997). *J. Biol. Chem.* **272**, 22502–22508.
Hägerhäll, C. (1997). *Biochim. Biophys. Acta* **1320**, 107–141.
Hägerhäll, C., Friden, H., Aasa, R., and Hederstedt, L. (1995). *Biochemistry* **34**, 11080–11089.
Hames, B. D. (1990). *Gel Electrophoresis of Proteins: A Practical Approach*, Oxford University Press, p. 116–124.

Hastings, S. F., Kaysser, T. M., Jiang, F., Salerno, J., Gennis R. B., and Ingledew, W. J. (1998). *Eur. J. Biochem*. **255**, 317–323.
Hatchikian, E. C., and Legall, J. (1972). *Biochim. Biophys. Acta* **267**, 479–484.
Hirsch, C. A., Rasminsky, M., Davies, B. D., and Lin, E. C. C. (1963). *J. Biol. Chem.* **238**, 3770–3774.
Iverson, T. M., Luna-Chaves, C., Cecchini, G., and Rees, D. C. (1999). *Science* **284**, 1961–1966.
Iwata, S., Ostermeier, C., Ludwig, B., and Michel, H. (1995). *Nature* **376**, 660–669.
Janssen, S., Schäfer, G., Anemüller, S., and Moll, R. (1997). *J. Bacteriol*. **179**, 5560–5569.
Lancaster, C. R., Gross, R., Haas, A., Ritter, M., Mantele, W., Simon, J., and Kroger, A. (2000). *Proc. Natl. Acad. Sci. U.S.A.* **97**, 13051–13056.
Lancaster, C. R., Kroger, A., Auer, M., and Michel, H. (1999). *Nature* **402**, 377–385.
LeGall, J., and Fauque, G. (1988). Biology of Anaerobic Microorganism (Alexander J. E. Zehnder ed.), New York, pp. 586–639.
LeGall, J., Mazza, G., and Dragoni, N. (1965). *Biochem. Biophys. Acta* **99**, 385.
Lemos, R. S., Gomes, C. M., Santana, M., LeGall, J., Xavier, A. V., and Teixeira, M. (2001a). *FEBS Lett.* 40–43.
Lemos, R. S., Gomes, C. M., and Teixeira, M. (2001b). *Biochem. Biophys. Res. Commun.* **281**, 141–150.
Louro, R. O., Catarino, T., LeGall, J., Turner, D. L., and Xavier, A. V. (2001). *Chem. Biochem.* **2**, 831–837.
Louro, R. O., Pacheco, I., Turner, D. L., LeGall, J., and Xavier, A. V. (1996). *FEBS Lett.* **390**, 59–62.
Matsson, M., Tolstoy, D., Roland, A., and Hedersted, L. (2000). *Biochemistry* **39**, 8617–8624.
Miller, J. D., and Wakerley, D. S. (1966). *J. Gen. Microbiol.* **43**, 101–107.
Ohnishi, T., Moser, C. C., Page, C. C., Dutton, P. L., and Yano, T. (2000). *Structure* **8**, 23–32.
Page, C. C., Moser, C. C., Chen, X., and Dutton, P. L. (1999). *Nature* **402**, 47–52.
Papa, S. (1979). *Biochim. Biophys. Acta.* **456**, 39–84.
Peck, H. D., Jr. (1966). *Biochem. Biophys. Res. Commun.* **22**, 112–118.
Pereira, I. A. C., LeGall, J., Xavier, A. V., and Teixeira, M. (2000). *Biochim. Biophys. Acta* **1481**, 119–130.
Pereira, I. A. C., Teixeira, M., and Xavier, A. V. (1998). *Struct. Bonding* **91**, 135–159.
Pereira, I. C., Abreu, I. A., Xavier, A. V., LeGall, J., and Teixeira, M. (1996). *Biochem. Biophys. Res. Comm*. **224**, 611–618.
Pereira, I. C., LeGall, J., Xavier, A. V., and Teixeira, M. (1997). *J. Biol. Inor. Chem.* **2**, 23–31.
Pereira, M. M., Carita, J. N., and Teixeira, M. (1999). *Biochemistry* **38**, 1276–1283.
Romão, C. V., Pereira, I. A., Xavier, A. V., LeGall, J., and Teixeira, M. (1997). *Biochem. Biophys. Res. Commun.* **240**, 75–79.
Rothery, R. A., and Weiner, J. H. (1998). *Eur. J. Biochem.* **254**, 588–595.
Rothery, R. A., Blasco, F., Magalon, A., Asso, M., and Weiner, J. H. (1999). *Biochemistry* **38**, 12747–12757.
Samain, E., Patil, D. S., DerVartanian, D. V., Albagnac, G., and LeGall, J. (1987). *FEBS Lett*. **216**, 140–144.
Schirawski, J., and Unden, G. (1998). *Eur. J. Biochem.* **257**, 210–215.
Smirnova, I. A., Hägerhäll, C., Konstantinov, A. A., and Hederstedt, L. (1995). *FEBS Lett.* **359**, 23–26.
Soares, C., Martel, P., and Carrondo, M. A. (1997). *J. Biol. Inorg. Chem.* **2**, 714–727.
Spencer, M. E., and Guest, J. R. (1973). *J. Bacteriol.* **114**, 563–570.
Teixeira, M., Fauque, G., Moura, I., Lespinat, P. A., Berlier, Y., Prickril, B., Peck, H. D., Xavier, A. V., LeGall, J., and Moura, J. J. (1987). *Eur. J. Biochem.* **167**, 47–58.
Tsukihara, T., Aoyama, H., Yamashita, E., Tomizaki, T., Yamaguchi, H., Shinzawa-Itoh, K., Nakashima, R., Yaono, R., and Yoshikawa, S. (1995). *Science* **269**, 1069–1074.
Turner, D., Salgueiro, C., Catarino, T., LeGall, J., and Xavier, A. V. (1996). *Eur. J. Biochem.* **241**, 723–731.
Wallace, B. J., and Young, I. G. (1977). *Biochim. Biophys. Acta* **461**, 84–100.
Waters, C. (1978). *Anal. Biochem.* **70**, 241.
Xavier, A. V. (2000). Structural bases for redox-Bohr linked energy transduction. In *18th International Congress of Biochemistry and Molecular Biology*, Birmighan, UK, pp. 98.